Department of Mathematics

Applying the interior and exterior traces to the Stratton-Chu formulae, we arrive at the boundary integral equations [8]

$$\left(-\frac{1}{2}I + \mathbf{C}_{-}\right)\gamma_D^{-}\mathbf{E} + \mathbf{S}_{-}\gamma_N^{-}\mathbf{E} = 0 \tag{9}$$

$$-\mathbf{S}_i\gamma_D^{-}\mathbf{E} + \left(-\frac{1}{2}I + \mathbf{C}_{-}\right.$$

We note that the scattered far-field is transverse, $\hat{\mathbf{e}}^r \cdot \tilde{\mathbf{F}} = 0$, hence it may be written

$$\mathbf{E}^s = (E^s_{\parallel}\hat{\mathbf{e}}_{\parallel s} + E^s_{\perp}\hat{\mathbf{e}}^s_{\perp s})e^{ikr},$$

where (in the case $\phi = 0$)

$$\hat{\mathbf{e}}_{\parallel s} = \hat{\mathbf{e}}_{\vartheta}, \quad \hat{\mathbf{e}}_{\perp s} = \hat{\mathbf{z}}, \quad \hat{\mathbf{e}}_{\perp s} \times \hat{\mathbf{e}}_{\parallel s} = \hat{\mathbf{e}}_r,$$

following the notation of [7]. The BEM++ output far-field can be converted to this new form simply by the transformation

$$E^s_{\parallel s} = -\sin(\vartheta)E^s_x + \cos(\vartheta)E^s_y, \quad E^s_{\perp s} = E^s_z. \tag{20}$$

In a similar way, the incident field is written in terms of its frame as

$$\mathbf{E}^i = (E^i_{\parallel i}\hat{\mathbf{e}}_{\parallel i} + E^i_{\perp i}\hat{\mathbf{e}}_{\perp i})e^{ikx},$$

where, in this case,

$$\hat{\mathbf{e}}_{\parallel i} = \hat{\mathbf{y}} \quad \text{and} \quad \hat{\mathbf{e}}_{\perp i} = \hat{\mathbf{z}}.$$

The *Amplitude Scattering Matrix* defines the relationship between the scattered far-field and the *arbitrarily polarised* incident field in their respective coordinate frames, i.e.

$$\begin{pmatrix} E^s_{\parallel s} \\ E^s_{\perp s} \end{pmatrix} = \frac{e^{ik(r-x)}}{-ikr}\begin{pmatrix} A_{11} & A_{12} \\ A_{21} & A_{22} \end{pmatrix}\begin{pmatrix} E^i_{\parallel i} \\ E^i_{\perp i} \end{pmatrix} \tag{21}$$

In order to calculate all entries A_{ij}, we consider two separate incident waves with different polarisations: one polarised in the $\hat{\mathbf{z}}$-direction and the other polarised in the $\hat{\mathbf{y}}$-direction. Each wave has unit amplitude and travels in the positive x-direction, as depicted in Figure 1. Let us consider these two problems separately.

4.1.1. $\hat{\mathbf{z}}$-polarised incident wave

In this case the incident wave has the form

$$\mathbf{E}^i = (1 \cdot \hat{\mathbf{e}}_{\perp i} + 0 \cdot \hat{\mathbf{e}}_{\parallel i})e^{ikx}$$

and thus it is possible to calculate two of the matrix entries, namely A_{12} and A_{22}. They are given as

$A_{12} = -\sin(\vartheta)E^s_x + \cos($

where p is the *phase function* $p = \mathbf{P}/4\pi$.

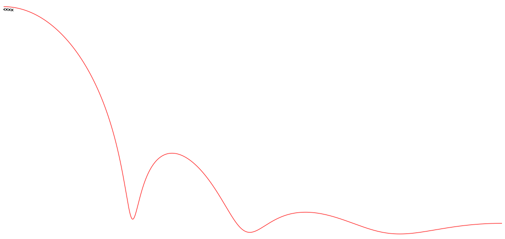
xxxx

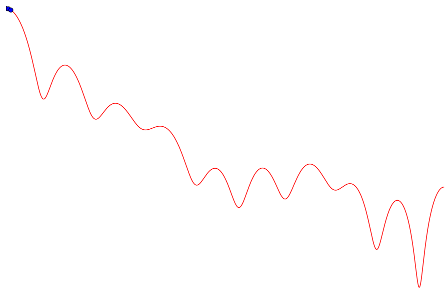

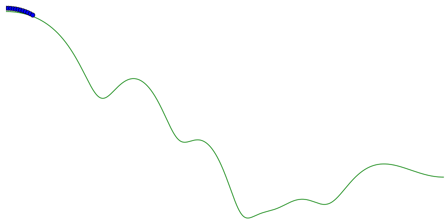

of 1% is required. If a lower accuracy is required, or a larger machine is available, this size parameter range can of course be extended. Also, it should be noted that BEM++ is not exploiting the symmetries of the shape to reduce memory consumption as is done in [19, 24]. Hence, for non-symmetrical shapes, we can expect a similar size parameter range of application.

We demonstrated that, although the scattering and extinction efficiencies differed from those of the T-matrix by approximately 1%, the phase matrix entries were vir-

acp-8-1609-2008.
[17] K. N. Liou. Influence of cirrus clouds on weather and climate processes: A global perspective. *Mon. Weather Rev.*, 114(6): 1167–1199, 1986.
[18] A. Macke, J. Mueller, and E. Raschke. Single scattering properties of atmospheric ice crystals. *J. Atmos. Sci.*, 53(19):2813–2825, 1996.
[19] Y. Mano. Exact solution of electromagnetic scattering by a three-dimensional hexagonal ice column obtained with the boundary-element method. *Appl. Optics*, 39(30):5541–5546, 2000.
[20] P. A. Martin and P. Ola. Boundary integral equations for the scattering of electromagnetic waves by a homogeneous dielectric obtacle. *Proc. Roy. Soc. Edinburgh*, 123A:185–208, 1993.
[21] J. R. Mautz and R. F. Harrington. Electromagnetic scattering from a homogeneous material body of revolution. *Archiv Elektronik und Uebertragungstechnik*, 33:71–80, 1979.
[22] M. I. Mishchenko and L. D. Travis. Capabilities and limitations of a current FORTRAN implementation of the T-matrix method for randomly oriented, rotationally symmetric scatterers. *J. Quant. Spectrosc. Ra.*, 60(3):309–324, 1998.
[23] Karri Muinonen. Scattering of light by crystals: a modified kirchhoff approximation. *Appl. Optics*, 28(15):3044–3050, 1989.
[24] T. Y. Nakajima, T. Nakajima, Yoshimori K., S. K. Mishra, and S. N. Tripathi. Development of a light scattering solver applicable to particles of arbitrary shape on the basis of the surface-integral equations method of Müller type. I. methodology, accuracy of calculation, and electromagnetic current on the particle surface. *Appl. Optics*, 48(19):3526–3536, 2009.
[25] J. C. Nédélec. *Acoustic and Electromagnetic Equations: Integral Representations for Harmonic Problems*. Springer, New York, 2001.
[26] Kenneth Sassen, Zhien Wang, and Dong Liu. Global distribution of cirrus clouds from CloudSat/Cloud-Aerosol lidar and infrared pathfinder satellite observations (CALIPSO) measurements. *J. Geophys. Res.-Atmos.*, 113(D8), 2008.
[27] W. Śmigaj, T. Betcke, S. Arridge, J. Phillips, and M. Schweiger. Solving boundary integral problems with BEM++. *ACM T. Math. Software*, 2015. doi: 10.1145/2590830.
[28] H. R. Smith, A. Webb, P. Connolly, A. J. Baran, A. R. D. Smedley, and E. Hesse. Cloud chamber laboratory investigations into the scattering properties of hollow ice particles. *J. Quant. Spectrosc. Ra.*, 157:106–118.
[29] W. Sun, Q. Fu, and Z. Chen. Finite-difference time-domain solution of light scattering by dielectric particles with a perfectly matched layer absorbing boundary condition. *Appl. Optics*, 38 (15):3141–3151, 1999.
[30] J. Um and G. M. McFarquhar. Single-scattering properties of aggregates of bullet rosettes in cirrus. *J. Appl. Meteor. Climatol.*, 46(6):757–775, 2007.